Two-Dimensional ^1H NMR Studies on HPr Protein from *Staphylococcus aureus*: Complete Sequential Assignments and Secondary Structure†

Hans Robert Kalbitzer,*,‡ Klaus-Peter Neidig,‡ and Wolfgang Hengstenberg§

Department of Biophysics, Max-Planck-Institute for Medical Research, Jahnstrasse 29, D-6900 Heidelberg, Germany, and Department of Biology, University of Bochum, D-4630 Bochum, Germany

Received June 3, 1991; Revised Manuscript Received August 28, 1991

ABSTRACT: Complete sequence-specific assignments of the ^1H NMR spectrum of HPr protein from *Staphylococcus aureus* were obtained by two-dimensional NMR methods. Important secondary structure elements that can be derived from the observed nuclear Overhauser effects are a large antiparallel β-pleated sheet consisting of four strands, A, B, C, D, a segment S_{AB} consisting of an extended region around the active-center histidine (His-15) and an α-helix, a half-turn between strands B and C, a segment S_{CD} which shows no typical secondary structure, and the α-helical, C-terminal segment S_{term}. These general structural features are similar to those found earlier in HPr proteins from different microorganisms such as *Escherichia coli*, *Bacillus subtilis*, and *Streptococcus faecalis*.

The phosphocarrier protein HPr[1] is an essential constituent of the phosphoenolpyruvate-dependent phosphotransferase system (PTS) that actively transports carbohydrates across the cell membrane of bacteria. It transfers a phosphonate group from enzyme I to enzyme III (factor III); the phosphonate group is transiently bound to the N1 atom of its active-center histidine (His-15) (Anderson et al., 1971; Gassner et al., 1977; Doijewaard et al., 1979; Kalbitzer et al., 1982). The X-ray structure of HPr protein from *Escherichia coli* has been solved (El-Kabbani et al., 1987; Waygood et al., 1989); it is very different from the solution structure determined by NMR for HPr from *E. coli* (Klevit & Drobny, 1986; Klevit et al., 1986; Klevit & Waygood, 1986; Waygood et al., 1989). Subsequently, the existence of an important secondary structure motive, a four-stranded antiparallel β-sheet found in the NMR structure of HPr from *E. coli* but not in the crystal structure, was confirmed also in the NMR structures of homologous proteins from different Gram-positive bacteria, namely, in HPr from *Streptococcus faecalis* (Glaser, 1987; Hengstenberg et al., 1989; Lorenz, 1990), *Bacillus subtilis* (Wittekind et al., 1989, 1990), and *Staphylococcus aureus* (Kalbitzer et al., 1990). The HPr proteins of Gram-negative bacteria such as *E. coli* are only poor substitutes for HPr proteins from Gram-negative bacteria in mixed complementation assays (Hengstenberg et al., 1990), suggesting that there must be important structural differences between the recognition site of HPr for enzyme I and/or for enzyme III. In contrast, HPr proteins of Gram-negative microorganism can replace each other, although they exhibit only a moderate sequence homology (compared to HPr from *S. aureus*: HPr from *S. faecalis* 65%, HPr from *S. subtilis* 61%, and HPr from *E. coli* 32%). Solving the NMR structures of this group of homologous proteins may make it possible to separate important structural features from more accidental ones as an ultimate goal. In this paper, we will report the complete ^1H

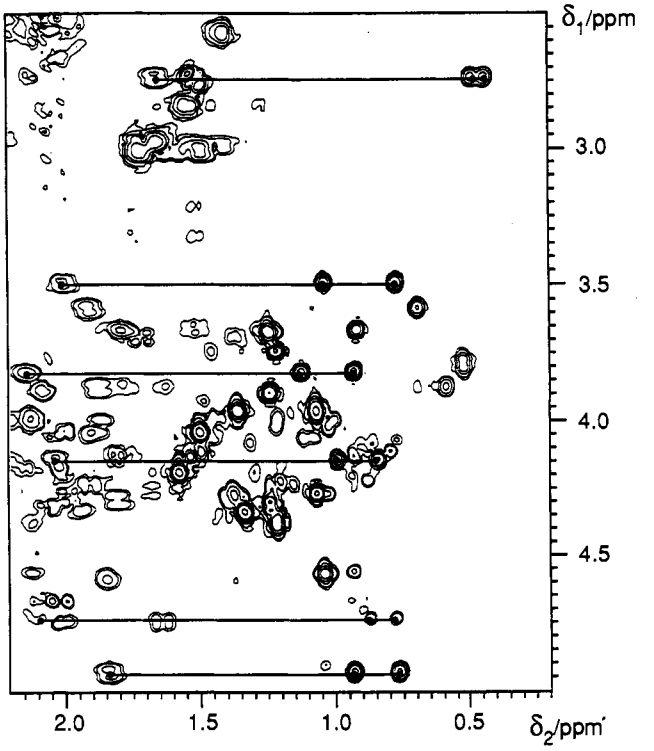

FIGURE 1: Valine spin systems in HPr protein *S. aureus*. Part of a 500-MHz ^1H NMR RCT spectrum of 4.9 mM HPr protein in D_2O at 308 K, pH 7.8. A total of 512 × 1024 time domain data points, sine multiplication in t_1 and t_2 direction, data size after Fourier transformation 1024 × 1024, representation in the absolute value mode. The Hα–Hβ and Hα–Hγ cross-peaks of the six valine spin systems occurring in the protein are indicated.

† Presented at the 14th International Conference on Magnetic Resonance in Biological Systems, Leicester, Great Britain.

‡ Max-Planck-Institute for Medical Research.

§ University of Bochum.

[1] Abbreviations: *B. subtilis*, *Bacillus subtilis*; DQF-COSY, double-quantum-filtered correlated spectroscopy; *E. coli*, *Escherichia coli*; HPr, heat-stable protein; DSS, 4,4-dimethyl-4-silapentanesulfonic acid; NMR, nuclear magnetic resonance; NOE, nuclear Overhauser effect; NOESY, nuclear Overhauser effect spectroscopy; PTS, phosphoenolpyruvate-dependent phosphotransferase system; RCT, relayed coherence transfer; *S. carnosus*, *Staphylococcus carnosus*; *S. aureus*, *Staphylococcus aureus*; *S. faecalis*, *Streptococcus faecalis*; TQF-COSY, triple-quantum-filtered correlated spectroscopy; TOCSY, total correlation spectroscopy.

0006-2960/91/0430-11186$02.50/0

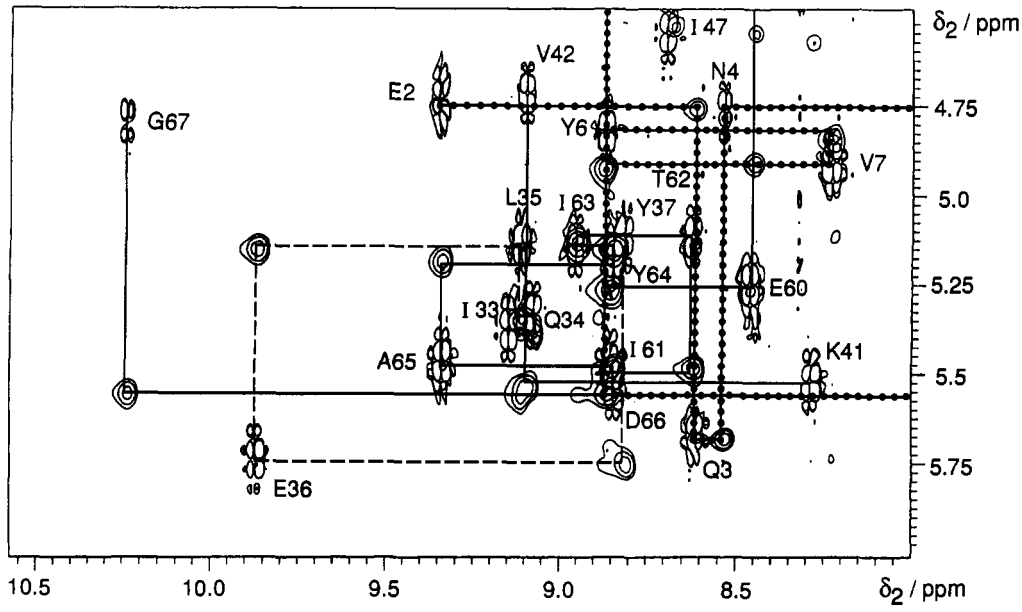

FIGURE 2: Sequential NOEs. Superposition of a 500-MHz ^{1}H NMR DQF-COSY and NOESY spectrum of HPr protein in water (95% H_2O/5% D_2O) at 308 K, pH 7.8. A total of 512 × 1024 time domain data points, sine multiplication in t_1 and t_2 direction, data size after Fourier transformation 1024 × 1024, phase-sensitive representation.

NMR assignments and the secondary structure of HPr from *S. aureus*.

Materials and Methods

Isolation of HPr Protein and Sample Preparation. HPr protein from *S. aureus* was isolated as described by Kalbitzer et al. (1982). NMR samples contained 4.9 mM HPr protein and 0.05 mM EDTA in 500 μL of D_2O or 500 μL of 95% H_2O/5% D_2O. Prior to sample preparation, oxygen was removed by flushing the solvents with helium and by storing the freeze-dried protein under helium atmosphere for several hours. After the protein was dissolved in the oxygen-free solvent, it was transferred to the sample tube, which was then sealed off under the helium atmosphere. The ^{1}H chemical shifts were referred to the internal reference 4,4-dimethyl-4-silapentanesulfonic acid (DSS). The pH value of the solution was adjusted to 7.8 by adding KOD to the solution. The pH value was measured with a combination glass electrode and was not corrected for isotope effects.

NMR Measurements. ^{1}H NMR spectra were recorded with a Bruker AM-500 NMR spectrometer operating at 500 MHz. The water signal was suppressed by selective presaturation. DQF- and TQF-COSY spectra were recorded according to Rance et al. (1983). Homonuclear RCT spectra were obtained as described by Eich et al. (1982) and Bax and Drobny (1985) with a total mixing time of 34 ms. The z-filtered TOCSY experiments were performed according to Braunschweiler and Ernst (1983) and Rance (1987) using Waltz-16 sequences (Shaka et al., 1983) of 70-, 100-, and 140-ms duration for isotropic mixing. NOESY spectra (Jeener et al., 1979) were recorded with a mixing time of 100 ms. In all experiments, phase-sensitive detection in the t_1 direction was obtained using time-proportional phase increments (TPPI) (Marion & Wüthrich, 1983). Typical recording times for two-dimensional spectra were 24–48 h. The data were evaluated with the program AURELIA.

Results

Assignments of Resonance Lines. The resonance lines were assigned essentially according to the procedure originally proposed by Wüthrich and co-workers [see, e.g., Wüthrich (1986)].

Assignments to Spin Systems. The complete spin systems of all glycine, alanine, threonine, phenylalanine, tryosine, and histidine residues could be identified unequivocally from the DQF-COSY, TQF-COSY, RCT, and TOCSY spectra. As an example for these assignments, a part of an RCT spectrum is shown in Figure 1 which contains the typical intense pairs of Hβ–Hγ COSY cross-peaks together with the corresponding Hα–Hγ RCT peaks. The spin systems of the protons of the three tyrosines, the histidine, and the phenylalanine rings were assigned earlier by one-dimensional methods (Rösch et al., 1981; Kalbitzer et al., 1982). The complete spin systems of the remaining amino acids were identified only after the sequential assignment of the amide, Hα, and Hβ resonances.

Sequential Assignments. Only one histidine, one phenylalanine, one arginine, and one proline residue occur in HPr from *S. aureus*; therefore, the sequential assignment of these spin systems should be trivial. However, as is often the case, the spin systems of arginine and proline could not be identified unequivocally in the first stage of evaluation (see above). For the remaining spin systems, a first hypothesis was usually formulated from the sequential NOEs, the amide–Hα cross-peaks in the COSY spectra, and the amide–Hα and the amide–Hβ cross-peaks in the RCT spectra. This hypothesis was confirmed by identifying the rest of the spin systems in the complete data set, that is, in DQF-COSY, RCT, TOCSY, and NOESY spectra in H_2O and D_2O (Table I). As an example, Figure 2 shows a region of the spectrum where strong sequential Hα–amide NOEs can be observed. Figure 3 summarizes the most important sequential and medium-range NOEs found. An interesting case is the Hγ of the hydroxyl group of Ser-31 that exchanges slowly enough to be observable: the measurements in H_2O show an additional Hβ1–Hγ cross-peak in the DQF-COSY and RCT spectra as well as an Hβ2–Hγ RCT cross-peak. These cross-peaks disappear in D_2O.

NOEs Defining the β-Pleated Sheet. The observation of strong sequential Hα–amide NOEs and the absence of sequential amide–amide NOEs in some parts of the sequence (Figures 2 and 3) suggest that these parts form a β-pleated

Table I: Sequential Assignments of the ^{1}H NMR Resonances of HPr from *S. aureus* at pH 7.8 and 308 K[a]

	chemical shift (ppm) relative to DSS						
residue	H	Hα	Hβ	Hγ	Hδ	Hε	Hζ
Met-1	*b*	4.71	2.12	2.51		2.06	
			2.18	2.61			
Glu-2	9.35	4.73	1.64	2.14			
			2.01	2.26			
Gln-3	8.61	5.66	1.49	2.02		6.70	
			1.89	2.02		7.30	
Asn-4	8.53	4.75	2.42		6.18		
			2.50		6.77		
Ser-5	7.87	5.55	3.48				
			3.86				
Tyr-6	8.87	4.82	2.25		6.86	6.53	
			2.98		6.86	6.53	
Val-7	8.23	4.91	1.84	0.76			
				0.92			
Ile-8	8.87	4.68	2.38	0.89 (γ2)	0.47		
				1.08			
				1.68			
Ile-9	7.93	4.24	1.65				
Asp-10	6.54	4.53	2.70				
			2.79				
Glu-11	8.67	3.88	2.07	2.34			
			2.07	2.34			
Thr-12	9.22	4.26	3.98	1.06			
Gly-13	8.19	3.11					
		4.36					
Ile-14	7.58	3.87	1.86	0.57 (γ2)	0.57		
				0.68			
				1.38			
His-15	6.73	4.73	3.03		7.25	7.81	
			3.36				
Ala-16	8.00	4.27	1.37				
Arg-17	8.07	4.27	1.89	1.49	3.21		
			1.96	1.72	3.33		
Pro-18	*b*	4.00	1.86	1.70	3.16		
			2.10	1.85	3.45		
Ala-19	8.06	3.66	1.23				
Thr-20	8.06	3.74	4.37	1.21			
Met-21	7.86	3.74	1.89	1.69		2.00	
			2.01	1.69			
Leu-22	8.89	4.06	1.10	1.89	0.83		
			1.46		0.89		
Val-23	8.22	3.48	1.98	0.76			
				1.03			
Gln-24	8.52	4.00	2.19	2.28			
			2.22	2.28			
Thr-25	7.87	3.90	4.32	1.23			
Ala-26	8.62	3.95	1.35				
Ser-27	8.05	4.11	4.03				
			4.34				
Lys-28	7.36	4.00	1.39	1.25	1.52	2.82	
			1.44	1.57	1.55	2.82	
Phe-29	7.43	4.51	2.76		7.38	7.16	7.07
			3.40		7.38	7.16	
Asp-30	11.27	4.49	2.58				
			2.68				
Ser-31	9.12	4.30	3.25	5.56			
			3.46				
Asp-32	7.87	4.53	2.56				
			2.60				
Ile-33	9.15	5.37	1.44	0.79 (γ2)	0.84		
				0.61			
Gln-34	9.07	5.34	1.74	2.11			
			2.01	2.26			
Leu-35	9.11	5.13	1.45	1.52	0.73		
			1.57		0.78		
Glu-36	9.87	5.74	2.12	1.87			
			2.36	1.95			
Tyr-37	8.81	5.10	2.66		7.24	6.96	
			3.11		7.24	6.96	
Asn-38	9.32	4.13	1.48				
			2.74				
Gly-39	8.45	5.33					
		5.42					
Lys-40	7.81	4.57	1.82	1.34	1.71	3.00	
			1.82	1.42	1.71	3.00	

Table I (Continued)

	chemical shift (ppm) relative to DSS						
residue	H	Hα	Hβ	Hγ	Hδ	Hε	Hζ
Lys-41	8.28	5.52	1.56	1.18	1.39	2.58	
			1.69	1.18	1.39	2.58	
Val-42	9.09	4.71	2.09	0.76			
				0.85			
Asn-43	7.51	5.10	2.76				
			3.49				
Leu-44	7.15	4.22	1.90				
			2.18				
Lys-45	7.79	3.82	1.78	1.45	1.52	2.74	
			2.40	1.45	1.52	2.74	
Ser-46	7.56	4.78	3.77				
			4.21				
Ile-47	8.69	4.55	2.11	0.92 (γ2)	0.70		
				0.81			
				1.22			
Met-48	8.45	4.12	0.88	1.68		2.10	
			1.80	2.18			
Gly-49	8.68	3.65					
		4.07					
Val-50	8.21	4.15	2.02	0.83			
				0.98			
Met-51	7.53	4.30	1.93	2.52		2.06	
			2.05	2.55			
Ser-52	8.51	3.87	1.62				
			1.77				
Leu-53	7.88	4.27	1.32	1.62	0.77		
			1.38		0.82		
Gly-54	7.82	3.98					
		4.06					
Val-55	8.11	2.75	1.64	0.44			
				0.48			
Gly-56	7.68	3.64					
		4.43					
Lys-57	7.86	3.64	1.52	1.11	1.51	3.02	
			2.16	1.90	1.51	3.02	
Asp-58	8.78	4.23	2.87				
			3.10				
Ala-59	7.55	4.33	1.32				
Glu-60	8.46	5.25	1.97	2.28			
			2.12	2.28			
Ile-61	8.85	5.47	1.95	0.90 (γ2)	0.63		
				0.99			
				1.68			
Thr-62	8.62	5.11	3.80	0.51			
Ile-63	8.95	5.13	1.73	0.77 (γ2)	0.68		
				1.11			
				1.51			
Tyr-64	8.85	5.18	2.69		6.97	6.68	
			3.03		6.97	6.68	
Ala-65	9.34	5.47	1.16				
Asp-66	8.84	5.54	2.52				
			2.90				
Gly-67	10.23	3.96					
		4.81					
Ser-68	7.14	3.76	3.64				
			3.64				
Asp-69	8.06	4.60	2.87				
			3.08				
Glu-70	7.99	4.15	1.87	2.65			
			2.57	2.75			
Ser-71	8.23	4.14	3.84				
			3.90				
Asp-72	7.59	4.28	2.69				
			2.72				
Ala-73	8.28	2.08	0.69				
Ile-74	7.58	3.66	1.77	0.90 (γ2)	0.61		
				1.24			
				1.40			
Gln-75	7.29	3.98	2.09	2.40		7.08	
			2.35	2.53		8.22	
Ala-76	7.91	4.18	1.56				
Ile-77	8.23	3.58	1.89	0.67 (γ2)	1.04		
				0.96			
				1.09			
Ser-78	8.54	4.07	4.19				
			4.19				

Table I (Continued)

residue	chemical shift (ppm) relative to DSS						
	H	Hα	Hβ	Hγ	Hδ	Hε	Hζ
Asp-79	7.97	4.43	2.68				
			2.82				
Val-80	7.84	3.80	2.14	0.92			
				1.12			
Leu-81	8.02	3.68	1.36	1.47	−0.18		
			1.70		0.45		
Ser-82	7.44	4.35	3.92				
			3.92				
Lys-83	8.78	4.03	1.88	1.54	1.66	2.97	
			2.00	1.54	1.66	2.97	
Glu-84	8.18	4.28	1.79	2.25			
			2.35	2.51			
Gly-85	7.52	3.76					
		3.88					
Leu-86	8.08	4.48	1.95				
			2.30				
Thr-87	7.33	4.89	4.56	1.03			

[a] 4.9 mM HPr from *S. aureus* in 95% H_2O/5% D_2O, temperature 308 K, pH 7.8.
[b] Resonance not identified.

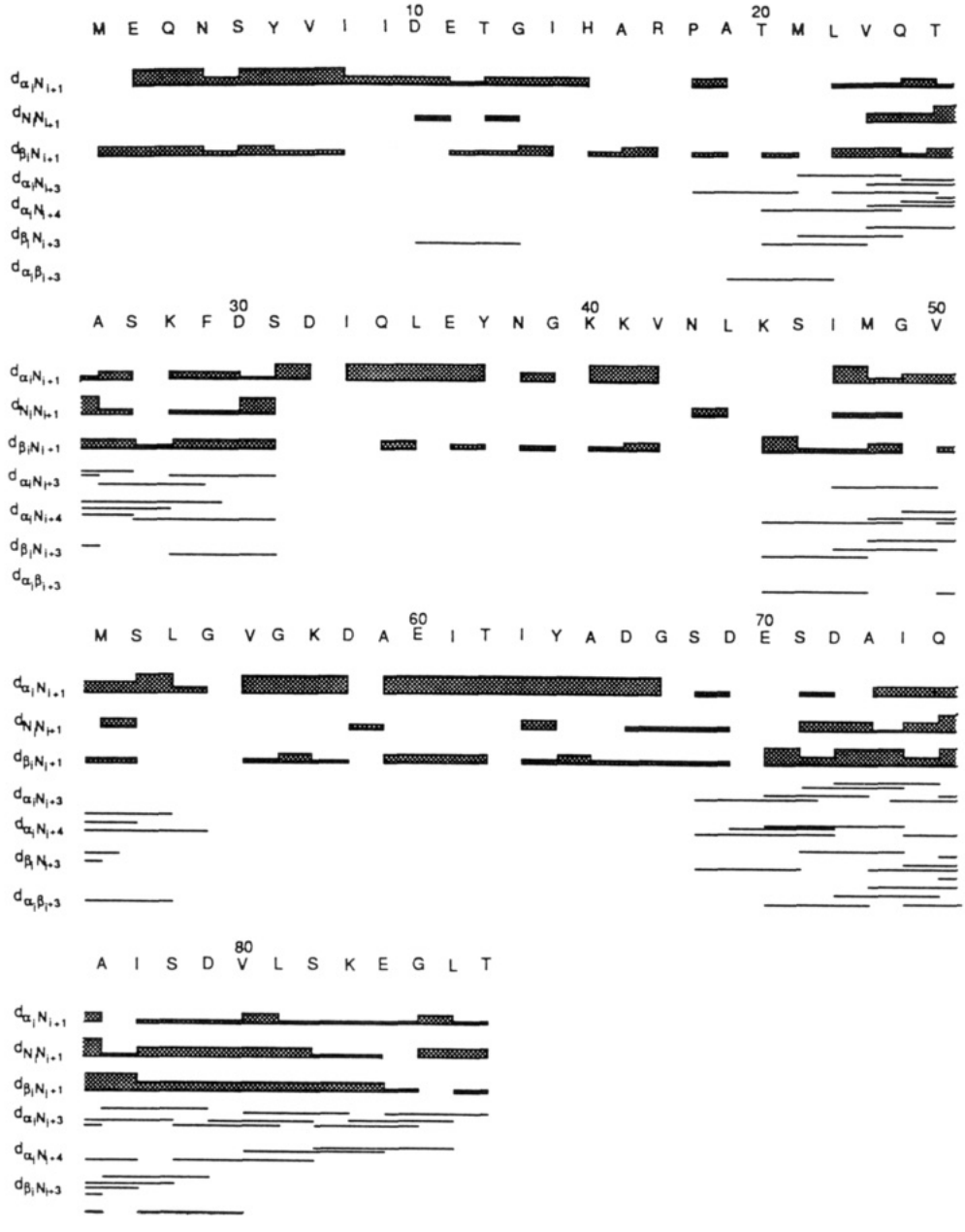

FIGURE 3: Schematic representation of the sequential and medium-range NOEs. Summary of the most important sequential NOEs, d_{xiyj}, between spin x in position i and spin y in position j. N, α, and β designate the amide, Hα, and Hβ atoms (spins), respectively. If NOEs to the two Hα spins of glycine were observed, the weaker NOE is represented as Hβ NOE.

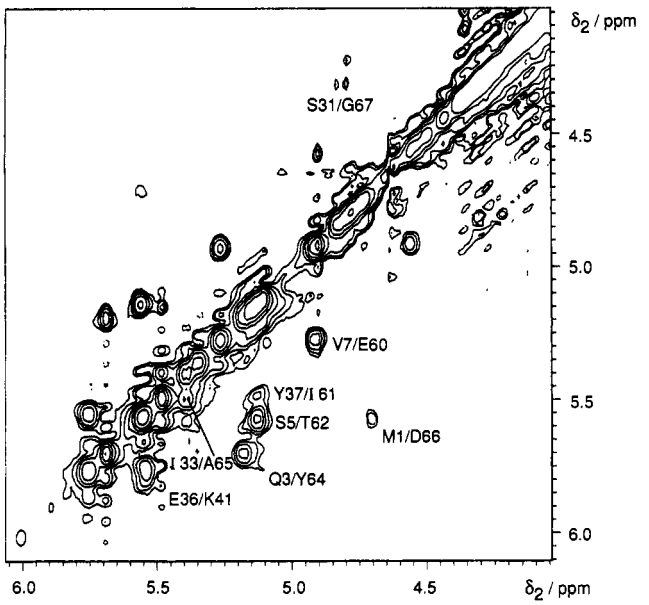

FIGURE 4: Hα–Hα NOEs in the β-pleated sheet region. Data were recorded using the same sample as in Figure 1. 500-MHz ^{1}H NMR NOESY spectrum of HPr protein in D_2O at 308 K, pH 7.8. A total of 512 × 1024 time domain data points, cosine multiplication in t_1 and t_2 direction, data size after Fourier transformation 1024 × 1024, phase-sensitive representation.

sheet. This is confirmed by the occurrence of characteristic NOEs between the strands of the sheet. Most important are the strong interstrand Hα–Hα NOEs observed (Figure 4), which are to be expected since in a regular antiparallel β-pleated sheet the Hα–Hα distance is approximately 0.23 nm. The observation of a network of additional interstrand amide–amide and amide–Hα NOEs completes the picture (Figure 5). As usual in NMR spectroscopy, not all cross-peaks expected from the distance map could be detected unambiguously. However, in many cases, good reasons for such an ambiguity can be given: (a) the chemical shifts of the atoms concerned are similar (the corresponding NOE cross-peak is located on or near the diagonal); (b) the cross-peaks are located in a crowded region (superposition with other cross-peaks prevents the unequivocal identification); or (c) the cross-peaks are too weak to be observed (exchange broadening, saturation of faster exchanging amide proton resonances, or direct saturation of the Hα resonance as suggested by the observation of an RCT, but not a COSY amide–Hα cross-peak). Therefore, Figure 5 shows not only the unequivocally identified NOEs (solid lines) but also such NOEs which may exist but cannot be observed definitely (dashed lines).

Discussion

The sequential assignments of the three tyrosine residues have been previously achieved by selective nitration (Rösch et al., 1981; Kalbitzer et al., 1985; Hausser & Kalbitzer, 1989). However, in the originally published sequence data (Beyreuther et al., 1977), 17 amino acids were missing (Hengstenberg et al., 1989), so that the sequential assignments from Rösch et al. (1981) and Kalbitzer et al. (1985) had to be adapted to the revised sequence (Hausser & Kalbitzer, 1991). Val-7 could be identified by comparison of the spectra from *S. aureus* with the homologous protein from *S. carnosus* where Val-7 is replaced by a threonine residue (Hausser & Kalbitzer, 1991). All these sequential assignments could be independently confirmed by the existence of the corresponding sequential NOEs.

From the NOE pattern, the existence of an antiparallel four-stranded β-pleated sheet in HPr from *S. aureus* can be derived unequivocally. The four β-strands A, B, C, and D comprise amino acids 1–8, 31–37, 40–43, and 59–67 (Figure 4). Strands B and C are connected by a half-turn. The regular structure at the end of strand C appears to be somewhat disturbed, since no sequential Hα–amide NOE between residues 42 and 43 and no Hα–Hα interstrand NOE between residues 43 and 34 could be observed. The same arrangement of β-strands has been reported for HPr proteins from *E. coli* (Klevit & Waygood, 1986), from *S. faecalis* (Glaser, 1987; Lorenz, 1990), and from *B. subtilis* (Wittekind et al., 1990).

The β-strands A and B are linked by the segment S_{AB} and the β-strands C and D by the segment S_{CD}; the β-strand D is followed by the C-terminal segment S_{term}. The first part of segment S_{AB} shows almost no medium-range NOEs but shows Hα–amide NOEs, indicating an extended structure; beginning with Pro-18, medium-range NOEs suggest a more compact structure, and from Leu-22 onward, the NOE pattern is typical of an α-helical conformation. Ser-31, which is located at the transition between β-strand B and segment S_{AB}, shows the unusual feature that its hydroxyl proton exchanges so slowly that it can be directly observed (Table I). It must be involved in very strong hydrogen bonding or be shielded completely from the bulk water. A rather compact pattern is also found for segment S_{CD}, but the sequential amide–amide NOEs typical of a regular α-helical structure are only found in very short stretches of the sequence. The C-terminal seg-

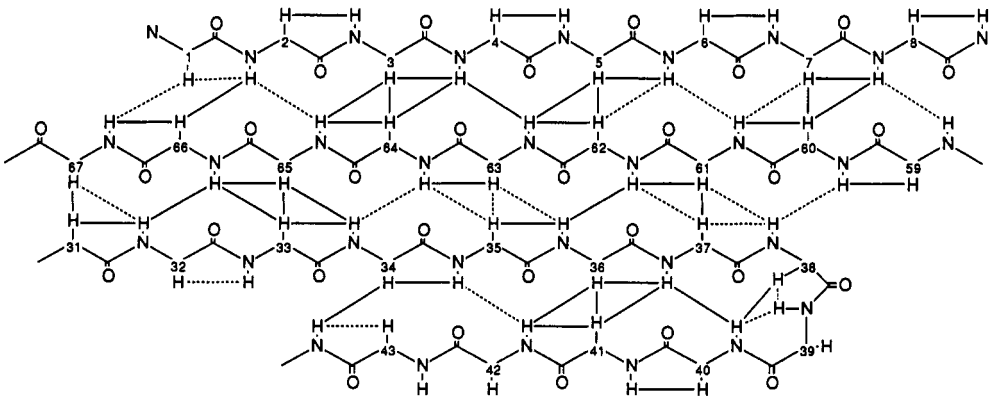

FIGURE 5: Four-stranded antiparallel β-pleated sheet in HPr protein. Schematic view of the β-pleated sheet in HPr protein and the network of inter- and intrachain Hα–Hα, Hα–amide, and amide–amide NOEs. Solid lines represent unambiguously observed NOEs; dashed lines represent expected NOEs which may exist but cannot be identified unequivocally because of superposition with other cross-peaks, degeneracy of chemical shifts, or line broadening by chemical exchange (see Results).

ment S_{term} shows again the typical NOE pattern for α-helical structures. This picture agrees rather well with the secondary structures found in other HPr proteins, with exception of segment S_{CD} which is α-helical in HPr from *E. coli* (Klevit & Waygood, 1986) and shows only one turn of an α-helix in HPr from *B. subtilis* (Wittekind et al., 1990).

These structural differences in segment S_{CD}, which is in close contact to segment S_{AB} containing the active-center histidine (His-15), may explain functional differences between HPr proteins.

References

Anderson, B., Weigel, N., Kundig, W., & Roseman, S. (1971) *J. Biol. Chem. 246*, 7023–7033.

Bax, A., & Drobny, G. (1985) *J. Magn. Reson. 61*, 306–320.

Beyreuther, K., Raufuss, H., Schrecker, O., & Hengstenberg, W. (1977) *Eur. J. Biochem. 75*, 275–286.

Braunschweiler, L., & Ernst, R. R. (1983) *J. Magn. Reson. 53*, 521–528.

Deutscher, J., & Saier, M. H. (1983) *Proc. Natl. Acad. Sci. U.S.A. 80*, 6790–6794.

Deutscher, J., Kessler, U., & Hengstenberg, W. (1985) *J. Bacteriol. 163*, 1203–1209.

Doijewaard, G., Roosien, F. F., & Robillard, G. T. (1979) *Biochemistry 18*, 2996–3001.

Eich, G., Bodenhausen, G., & Ernst, R. R. (1982) *J. Am. Chem. Soc. 104*, 3731–3732.

El-Kabbani, O. A. L., Waygood, E. B., & Delbaere, L. T. J. (1987) *J. Biol. Chem. 262*, 12926–12929.

Gassner, M., Stehlik, D., Schrecker, O., Hengstenberg, W., Maurer, W., & Rüterjans, H. (1977) *Eur. J. Biochem. 75*, 287–296.

Glaser, S. (1987) Doctoral Thesis, Heidelberg.

Hausser, K. H., & Kalbitzer, H. R. (1991) *NMR in Medicine and Biology. Structure Determination, Tomography, In Vivo Spectroscopy*, Springer, New York.

Hengstenberg, W., Reiche, B., Eisermann, R., Fischer, R., Kessler, U., Tarrach, A., de Voss, W. M., Kalbitzer, H. R., & Glaser, S. (1989) *FEMS Microbiol. Rev. 63*, 35–42.

Jeener, J., Meier, B. H., Bachmann, P., & Ernst, R. R. (1979) *J. Chem. Phys. 71*, 4546–4553.

Kalbitzer, H. R., Deutscher, J., Hengstenberg, W., & Rösch, P. (1981) *Biochemistry 20*, 6178–6185.

Kalbitzer, H. R., Hengstenberg, W., Rösch, P., Muss, P., Bernsmann, P., Engelmann, R., Dörschug, M., & Deutscher, J. (1982) *Biochemistry 21*, 2879–2885.

Kalbitzer, H. R., Muss, H. P., Engelmann, R., Kiltz, H. H., Stüber, K., & Hengstenberg, W. (1985) *Biochemistry 24*, 4562–4569.

Kalbitzer, H. R., Neidig, K.-P., & Hengstenberg, W. (1990) *Physica B 164*, 180–192.

Klevit, R. E., & Drobny, G. P. (1986) *Biochemistry 25*, 7770–7773.

Klevit, R. E., & Waygood, E. B. (1986) *Biochemistry 25*, 7774–7781.

Klevit, R. E., Drobny, G. P., & Waygood, E. B. (1986) *Biochemistry 25*, 7760–7769.

Lorenz, M. (1990) Diploma Thesis, Heidelberg.

Marion, D., & Wüthrich, K. (1983) *Biochem. Biophys. Res. Commun. 113*, 967–974.

Rance, M. (1987) *J. Magn. Reson. 74*, 557–564.

Rance, M., Sorensen, O. W., Bodenhausen, G., Wagner, G., Ernst, R. R., & Wüthrich, K. (1983) *Biochem. Biophys. Res. Commun. 117*, 479–485.

Rösch, P., Kalbitzer, H. R., Schmidt-Aderjan, U., & Hengstenberg, W. (1981) *Biochemistry 20*, 1599–1605.

Shaka, A. J., Keeler, J., Frenkiel, T., & Freeman, R. (1983) *J. Magn. Reson. 52*, 335–338.

Waygood, E. B., Sharma, S., Bhanot, P., El-Kabbani, O. A. L., Delbaere, L. T. J., Georges, F., Wittekind, M. G., & Klevit, R. E. (1989) *Microbiol. Rev. 63*, 43–52.

Wittekind, M., Reizer, J., Deutscher, J., Saier, M. H., & Klevit, R. E. (1989) *Biochemistry 28*, 9908–9912.

Wittekind, M., Reizer, J., & Klevit, R. E. (1990) *Biochemistry 29*, 7191–7200.

Wüthrich, K. (1986) *NMR of Proteins and Nucleic Acids*, John Wiley, New York.